

# Carbon States in Carbon-Encapsulated Nickel Nanoparticles Studied by Means of X-Ray Absorption, Emission, and Photoelectron Spectroscopies

V. R. Galakhov,<sup>\*,†,‡</sup> A. Buling,<sup>¶</sup> M. Neumann,<sup>¶</sup> N. A. Ovechkina,<sup>†</sup> A. S. Shkvarin,<sup>†</sup>  
A. S. Semenova,<sup>§</sup> M. A. Uimin,<sup>†</sup> A. Ye. Yermakov,<sup>†</sup> E. Z. Kurmaev,<sup>†</sup>  
O. Y. Vilkov,<sup>||,⊥</sup> and D. W. Boukhvalov<sup>#</sup>

*Institute of Metal Physics, Russian Academy of Sciences — Ural Division, S. Kovalevskaya str.,  
18, 620990 Yekaterinburg, Russia, Ural State Mining University, Kuibyshev str., 30, 620144  
Yekaterinburg, Russia, Fachbereich Physik, Universität Osnabrück, Barbarastrasse 7, D-49069  
Osnabrück, Germany, Institute of Solid State Chemistry, Russian Academy of Sciences — Ural  
Division, Pervomayskaya str., 91, 620990 Yekaterinburg, Russia, Technische Universität Dresden,  
Germany, St. Petersburg State University, Russia, and School of Computational Sciences, Korea  
Institute for Advanced Study (KIAS) Hoegiro 87, Dongdaemun-Gu, Seoul, 130-722, Korean  
Republic*

E-mail: galakhov@ifmlrs.uran.ru

## Abstract

Electronic structure of nickel nanoparticles encapsulated in carbon was characterized by photoelectron, X-ray absorption, and X-ray emission spectroscopies. Experimental spectra are compared with the density of states calculated in the frame of the density functional theory. The carbon shell of Ni nanoparticles has been found to be multilayer graphene with significant (about 6%) amount of Stone–Wales defects. Results of the experiments evidence protection of the metallic nanoparticles from the environmental degradation by providing a barrier against oxidation at least for two years. Exposure in air for 2 years leads to oxidation only of the carbon shell of Ni@C nanoparticles with coverage of functional groups.

## Introduction

Metallic nanoparticles have potential applications in many technical and biological fields (drug delivery, cancer diagnostics, catalysis etc.).<sup>1–11</sup> In order to prevent metallic nanoparticles from oxidation and agglomerations upon thermal treatments, they are encapsulated in carbon.<sup>12–15</sup> Metallic nanoparticles wrapped in carbon layers can retain the intrinsic properties of metals at nanoscales.

Magnetic properties of these systems depend on sizes of the particles as well as their degree of crystallinity and the chemical state. Carbon-coated ferromagnetic metal nanoparticles are predominantly single domain and display the superparamagnetic behavior.<sup>11</sup> Moreover, the carbon coatings can endow magnetic particles with biocompatibility and stability in many organic and inorganic media.<sup>5–9,14</sup> The instability, large aggregation, and rapid biodegradation of the pure uncoated (naked) magnetic nanoparticles could be overcome by replacement of the naked magnetic nanoparticles by the encapsulated ones, since the intrinsic properties of the inner magnetic cores

---

\*To whom correspondence should be addressed

†Institute of Metal Physics

‡Ural State Mining University

¶Universität Osnabrück

§Institute of Solid State Chemistry

||Technische Universität Dresden

⊥St. Petersburg State University

#School of Computational Sciences

in this case are well protected by outer carbon shells, which in turn gives many possibilities for further modification. Besides, the combination of carbon coating and metallic cores having ‘core-shell’ structure provides unusual catalytic properties to these nanocomposites.<sup>13,14</sup> However, up to now, the nature of the catalytic activity of the mentioned nanoparticles is still an open question.

Initially, we have studied carbon encapsulated nickel and iron nanoparticles by means of X-ray absorption and photoelectron spectroscopy methods.<sup>16</sup> We have found that Fe and Ni cores are in metallic states and carbon coating protects the metallic nanoparticles from the environmental degradation. In the present paper we have concentrated the main attention for study of Ni@C nanoparticles. The previous studies are completed (i) by measurements of X-ray emission spectra (XES), (ii) by studies of Ni@C nanoparticles after 2 years storage, (iii) by calculations of the electronic structure of Ni@C using the density functional theory (DFT) for different models of carbon coating. We will show that the carbon shell of Ni nanoparticles can be described by multilayer graphene with some amount of Stone–Wales defects.

## **Experimental and calculation details**

Nanocomposites Ni@C were produced by evaporation of overheated ( $\sim 2000$  °C) Ni liquid drop by blowing up a buffer inert gas (Ar) containing a hydrocarbon as described in our earlier paper.<sup>16</sup> The melting of Ni drop performed by induction levitation system which provides clean conditions (no impurities and oxygen) for the obtained nanocomposites. The morphological characteristics and the structural parameters of the composites were analyzed by high-resolution transmission electron microscopy. Ni@C particles sizes are in the range of a few nanometers up to about 20 nm.

Our first spectral measurements were carried out within 2 days after preparing the Ni@C sample.<sup>16</sup> Replicates of the experiments were made after two years on the same Ni@C sample.

The C  $K\alpha$  X-ray emission spectrum (XES) was measured at the beamline 8.0.1 of the Advanced Light Source (ALS) at the Lawrence Berkeley National Laboratory. Photons were delivered to the sample via the beamline undulator insertion device and the spherical grating monochromator.

The measurements of X-ray absorption (XAS) and photoelectron (XPS) spectra of Ni@C were performed using the Multi User Stage for Angular Resolved Photoemission (MUSTANG) experimental station at the Russian–German beamline at BESSY equipped with a PHOIBOS 150 SPECS GmbH electron energy analyzer. The absorption spectra are registered in the total electron yield mode. The Ni 2p and C 1s XPS spectra for the as-prepared Ni@C sample [denoted as Ni@C (1)] were obtained at the photon energy of 950 eV. The valence-band photoelectron spectrum of Ni@C (1) was measured at the excitation energy of 200 eV.

X-ray photoelectron spectra for the Ni@C sample stored in air for 2 years [Ni@C (2)] were measured with an ESCA spectrometer from Physical Electronics (PHI 5600 ci) using monochromatic Al  $K\alpha$  radiation ( $h\nu = 1486.6$  eV).

We have measured also spectra of reference samples: Ni metal, NiO and highly oriented pyrolytic graphite (HOPG).

The calculations of the electronic structures of Ni@C nanoparticles were carried out with help of the density functional theory (DFT) using the pseudo potential SIESTA code,<sup>17,18</sup> within the framework of the local density approximation (LDA).<sup>19</sup> For the simulation of the atomic structure Ni@C nanoparticles, we have performed optimization of the geometric structure for several model systems, and then compared the obtained electronic structure with the experimental spectra.

## Results and discussion

Photoelectron spectroscopy is a feasible method for characterization of chemical states of materials and for providing information about the occupied electronic states. [figure][1][1] (a) shows valence-band photoelectron spectra measured for the as-prepared Ni@C nanoparticles [Ni@C (1)] (with excitation energy of 200 eV) and for the same sample stored in air for 2 years [Ni@C (2)] (with excitations energy of 1486.6 eV — Al  $K\alpha$  excitation line). For comparison, the spectra of Ni metal and NiO oxides measured at 1486.6 eV are shown.

According to data of Yeh and Lindau,<sup>20</sup> the electron photo-ionization cross-section ratios for

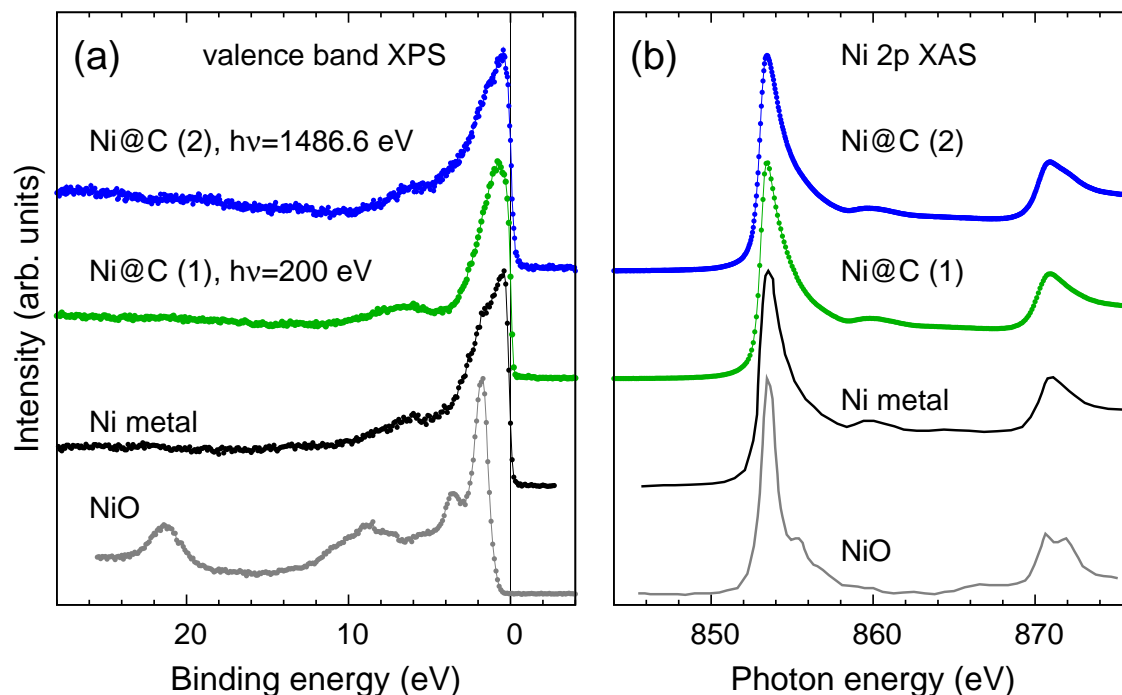


Figure 1: (a) Valence-band photoelectron spectra of as-prepared Ni@C nanoparticles (1) and Ni@C stored in air for 2 years (2) measured at the excitation energies 200 eV and 1486.6 eV, respectively. For comparison, the spectra of pure metals and oxides are shown. The spectra of Ni metal and NiO were measured at the excitations energy of 1486.6 eV. (b) Ni 2p X-ray absorption spectra of Ni@C nanoparticles, metallic Ni, and NiO.

Ni and C for the excitation energies of 200 eV and 1486.6 eV are equal to 110 and 590, respectively. Consequently the main contribution to the valence-band XPS spectrum in the presented energy region stems from the Ni 3d states. The similarity of the spectra of Ni metal and Ni@C demonstrates that Ni cores in Ni@C are in the metallic state.

In transition 3d metal compounds, cation 2p X-ray absorption spectra are dominated by intra-atomic and short-range effects. In view of this, metal 2p X-ray absorption spectra correspond to the metal 2p → metal valence band (3d) transitions and are determined by the valence state of metal atoms. [figure][1][1] (b) displays Ni 2p X-ray absorption spectra of the carbon-encapsulated Ni nanoparticles, Ni metal, and NiO. The Ni 2p X-ray absorption spectra of the carbon-encapsulated Ni nanoparticles are similar to those of metallic Ni. This means that Ni cores of as-prepared Ni@C (1) and Ni@C nanoparticles stored in air for 2 years (2) are in the metallic state.

These results demonstrate high efficiency of carbon protecting layers. Note, Cho et al.<sup>21</sup> found

that Au-coated Fe nanoparticles are oxidized after one month. Therefore carbon protects 3d metal against oxidation much better than gold.

Information about unoccupied carbon 2p states can be obtained from C 1s X-ray absorption spectra. C 1s X-ray absorption spectra of carbon encapsulated nanoparticles Ni@C and of HOPG are presented in [figure][2][2]. The spectra of HOPG are measured at two angles between the normal to the surface and of the synchrotron beam ( $\vartheta = 60^\circ$  and  $\vartheta = 0^\circ$ ). The measurements of the C 1s XAS spectra of HOPG at two orientations allow to separated  $\pi^*$  and  $\sigma^*$  states. The spectrum measured at  $\vartheta = 0^\circ$  reveals mainly  $\sigma^*$  states. The  $\pi^*$  states are seen in the spectrum measured at  $\vartheta = 60^\circ$ .

The C 1s XAS spectra of Ni@C are generally very similar to those of graphite, showing distinct  $\pi^*$  and  $\sigma^*$  bands (peaks *c*, *f*, and *g*), but with some noticeable exceptions. The spectra of Ni@C show peaks *a*, *b*, *d*, and *e* which are not exhibited in the spectra of graphite. Distinction between the C 1s XAS spectra of Ni@C and HOPG is seen in the insert to [figure][2][2] where the difference spectrum obtained by subtraction of the spectrum of HOPG (measured at  $\vartheta = 60^\circ$ ) from the spectrum of the as-prepared Ni@C sample is presented.

The features *a* and *b* located below the  $\pi^*$  resonance can be seen also in graphene C 1s XAS spectra.<sup>22–26</sup> These features are located a little lower than the Fermi level estimated from our C 1s X-ray photoelectron spectrum (284.5 eV). It was suggested<sup>22</sup> that the observed transition energy is determined by final state effects. Therefore, empty states can be observed below the Fermi level determined by XPS (see [figure][3][3]). An analogous peak in C 1s XAS of nanographite grains growth on Pt(111) was attributed to a zigzag edge-derived electronic state.<sup>22</sup> Hua et al.<sup>26</sup> showed that this peak is determined by defects and should not be present in an ideal graphene sheet. Note, an analogous feature at 284.5 eV (peak *b*) in the spectra of carbon nanotubes was attributed to the rolling (helicity) of the carbon layers of nanotubes.<sup>27</sup>

The peaks analogous to *d* and *e* in the spectra of Ni@C can be seen in the spectra of graphene<sup>24</sup> and, according to the work of Hua et al.,<sup>26</sup> these peaks should be explained by defects. Both  $\pi^*$  and  $\sigma^*$  resonances have contributions to these peaks. Note, that the intense features *d* and *e* are

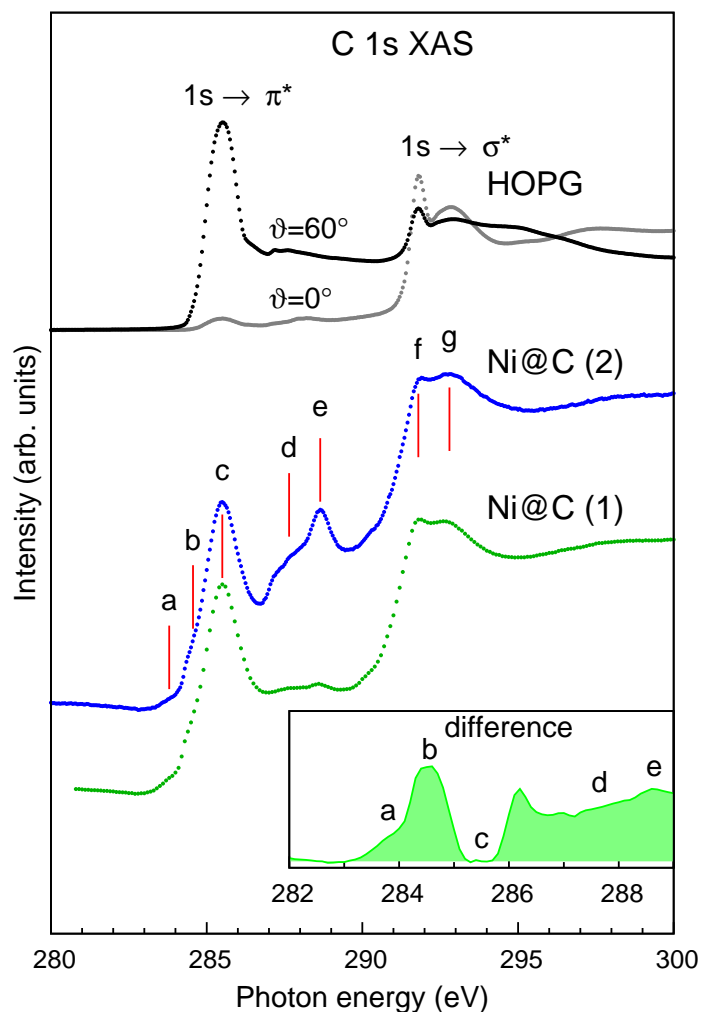


Figure 2: C 1s X-ray absorption spectra of HOPG and of as-prepared Ni@C nanoparticles (1) and Ni@C stored in air for 2 years (2). The spectra of HOPG are measured at two angles  $\vartheta$  between the normal to the surface of the samples and the X-ray beam. Insert shows the difference spectrum obtained by subtraction of the HOPG spectrum ( $\vartheta = 60^\circ$ ) from the spectrum of as-prepared Ni@C.

observed only for the Ni@C sample stored in air for 2 years. According to our X-ray photoelectron measurements, the sample Ni@C (2) is partly oxidized. Therefore, one should assigned these features to contaminations by a COOH group and/or C–H due to oxidation.<sup>28</sup>

The presence of functional groups in the Ni@C (2) nanoparticles can be confirmed by the C 1s photoelectron spectra shown in [figure][3][3]. The spectrum of as-prepared Ni@C (1) shows one C 1s peak at 284.5 eV with an asymmetric line shape attributed to  $sp^2$  bonded carbon atoms in reference to the XPS studies of graphite<sup>29</sup> or carbon nanotubes.<sup>30</sup> The C 1s XPS spectrum of Ni@C (2) is more complicated and, in order to separate signals from functional groups, we have

deconvoluted it into four peaks. As for Ni@C (1), the prominent peak at 284.5 eV reveals C–C interactions. The additional peaks in the C 1s XPS spectrum of Ni@C (2) at 285.5 eV, 286.6 eV, and 288.8 eV can be identified as hydroxyl (OH), carbonyl (C=O), and carboxyl (O=C–OH) groups attached to the carbon atom in Ni@C,<sup>31–34</sup> respectively, as it is shown in [figure][3][3]. The contributions of these functional groups to the C 1s XPS spectrum of Ni@C (2) are 19 %, 8 %, and 4 %, respectively.

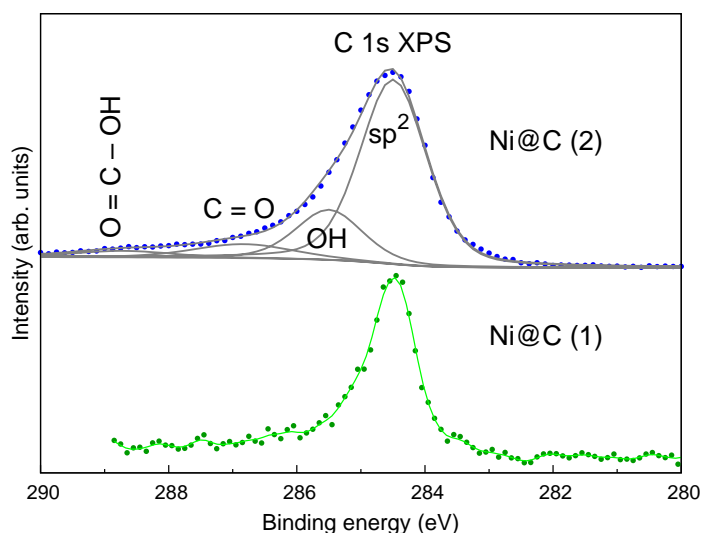


Figure 3: C 1s X-ray photoelectron spectra of as-prepared Ni@C nanoparticles (1) and Ni@C stored in air for 2 years (2). The spectra of the Ni@C (1) and Ni@C (2) samples are measured at the excitation energies of 950 eV and 1486.6 eV, respectively.

Calculations of the electronic structure of the carbon shell of Ni@C were carried out for a few layer graphene (FLG), i.e., 6 layers of graphene with Bernal (AB) stacking, one and three graphene layers on Ni (111). The starting geometric structure was taken from the work of Giovannetti et al.<sup>35</sup> Stone–Wales (SW) defects<sup>36</sup> were used in our model because of non-planarity of graphene layers folded around spherical particles. In order to examine the role of SW defects for the electronic structure the calculations for graphene monolayers containing a SW defect per 50 atoms in the supercell [[figure][4][4] (a)] have been performed. For imitation of the discussed defects in graphene multylayers we have used graphite containing SW defects in each layer [[figure][4][4] (b)]. The results of the calculations are presented in [figure][5][5].



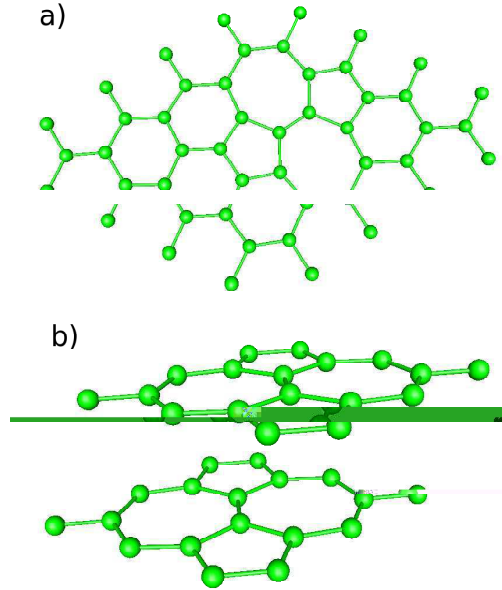


Figure 4: (a) The geometric structure optimized for graphene monolayer containing one Stone–Wales defect on supercell with 50 carbon atoms; (b) supercell of graphite with maximal concentration of Stone–Wales defects.

For comparison of the theoretical results with our experimental X-ray emission and absorption spectra, we have simulated the C 2p density of states of Ni@C as the sum of DOS for a graphene monolayer with SW defects multiplied by three and the DOS for three layers of graphene on Ni(111). The simulated DOS and experimentally measured C  $K\alpha$  X-ray emission (XES) and C 1s X-ray absorption (XAS) spectra of Ni@C (1) are presented in [figure][6][6]. C  $K\alpha$  X-ray emission spectra reveal the distribution of C 2p states in the occupied part of the valence band since they are appeared as a result of the  $2p \rightarrow 1s$  electronic transitions. These XAS and XES spectra for the as-prepared Ni@C sample plotted in the photon energy scale are given in the upper part of [figure][6][6]. The Fermi level estimated from the C 1s X-ray photoelectron spectrum (see [figure][3][3]) is shown by line. The  $K\alpha$  X-ray emission spectrum consists of a broad main peak at about 277 eV labeled by *A*, and a shoulder at about 282 eV labeled by *B*. Following the interpretation presented in the literature<sup>37,38</sup> one can attribute these features to  $\sigma$  and  $\pi$  orbitals, respectively. The combined use of the C  $K\alpha$  X-ray emission and C 1s X-ray absorption spectra

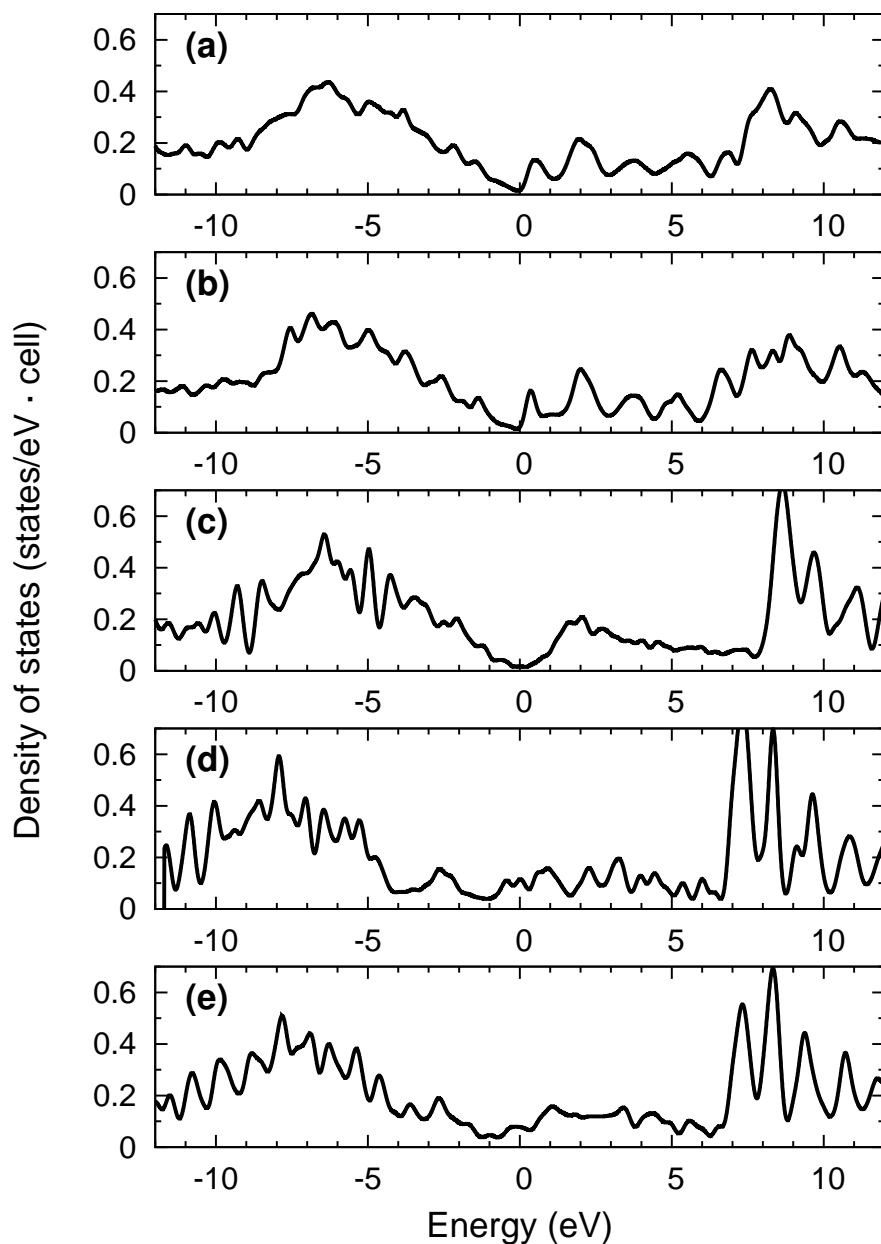


Figure 5: Densities of states of carbon for graphite and of a few layer of graphene on a single crystal of Ni(111) with and without Stone–Wales defects: (a) — graphite with SW defects; (b) — graphene monolayer with one SW defect; (c) — 6 layers of graphene; (d) — one layer of graphene on Ni (111); (e) — 3 layers of graphene on Ni (111).

(the upper part of [figure][6][16]) shows that there is no gap between the occupied and unoccupied C 2p states of Ni@C.

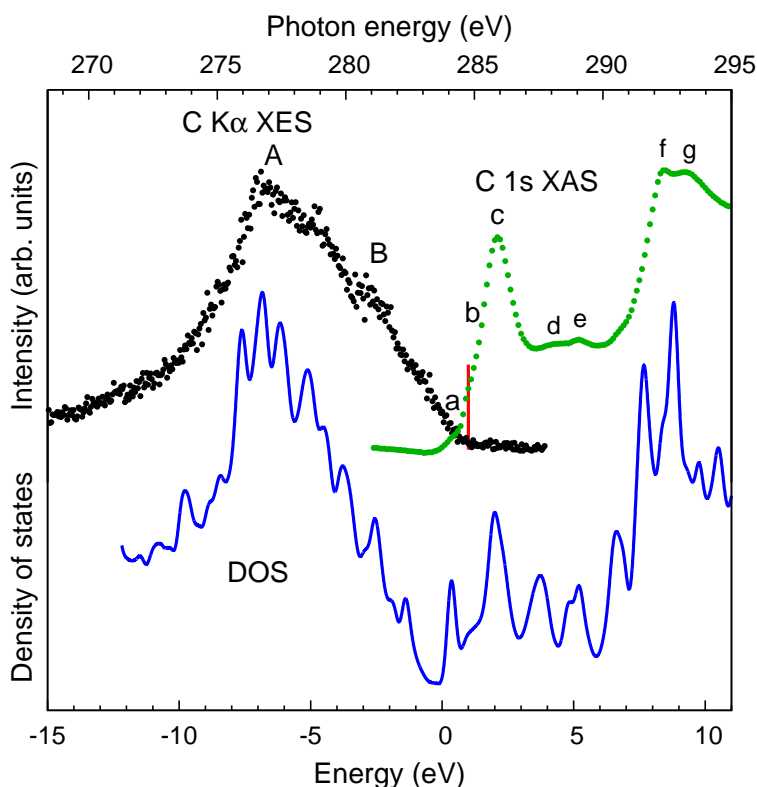


Figure 6: C  $K\alpha$  X-ray emission and C 1s X-ray absorption spectra of as-prepared Ni@C compared with density of states obtained for layer graphene on a single crystal of Ni(111) with Stone–Wales defects. The line shows the Fermi level estimated from the C 1s X-ray photoelectron spectrum.

One can see that the calculated superposition of the densities of states coincides well with the experimental C  $K\alpha$  emission and C 1s absorption spectra. Two additional features in the C 1s X-ray absorption spectrum near the Fermi level (features *a* and *b* in [figure][2][2]) are caused by the presence of SW defects [feature *a* at +0.5 eV — see also [figure][5][5] (a),(b)] and overlapping of the electronic states of graphene layers with those of the nickel substrate [feature *b* at about 1 eV — see [figure][5][5] (e)]. The comparison of the calculated density of states and C 1s XAS and C  $K\alpha$  XES spectra shows that the most appropriate structural model for the carbon coating of Ni@C particles is graphene multilayers with high concentration of SW defects (one per 18 carbon atoms — about 6 %) but some electronic contribution from the nearest to the Ni core carbon shells should be taken into account.

The similarity of C K $\alpha$  XES and C 1s XAS spectra of Ni@C ([figure][6][6]) with those of polymerized fullerene<sup>39,40</sup> evidences the presence of not only hexagonal but also pentagonal rings of carbon atoms. The presence of these defects leads to increased chemical activity of carbon encapsulated metals in comparison with that of flat carbon systems,<sup>41</sup> which is experimentally confirmed by surface oxidation of the Ni@C (2) sample. The appearance of Stone–Wales defects caused by spherical shape of the particles or reconstruction of the defects on the graphene-nickel interface was found experimentally<sup>42,43</sup> and theoretically.<sup>44</sup>

## Conclusions

In summary, we have studied the electronic and atomic structures of carbon-coated Ni nanoparticles by means of X-ray absorption, emission, and photoelectron spectroscopies and DFT calculations. Results of the measurements suggest that the atomic and electronic structures of Ni cores are similar to those of metallic Ni. Absence of any secondary phases and traces of oxidation of Ni after two years of exposure of Ni@C nanoparticles in air at ambient conditions confirms good protection properties of the carbon shell. Measurements of X-ray absorption and photoelectron spectra demonstrate some oxidation of the carbon shell. Comparison of experimental X-ray spectra and calculated densities of states points to the graphite-like structure of the carbon shell with significant amount (about 6%) of Stone–Wales defects. Some overlapping of the electronic states of graphene layers with those of Ni cores is also found.

## Acknowledgement

This work is supported by the Russian Foundation for Basic Research (grants 11-02-00166, 10-02-00323, and 11-02-00022), by the Program for Basic Research of the Russian Academy of Sciences “Physics of New Materials and Structures”, and by the bilateral Program “Russian–German Laboratory at BESSY”. DWB acknowledge computational support from the CAC of KIAS.

## References

- (1) Wu, X.; Liu, H.; Liu, J.; Haley, K. N.; Treadway, J. A.; Larson, J. P.; Ge, N.; Peale, F.; Bruchez, M. P. *Nature Biotechnology* **2002**, *21*, 41–46.
- (2) Paciotti, G.; Myer, L.; Weinreich, D.; Goia, D.; Pavel, N.; McLaughlin, R. E.; Tamarkin, L. *Drug Deliv.* **2004**, *11*, 169–183.
- (3) Alivisatos, P. *Nature Biotechnology* **2004**, *22*, 47–52.
- (4) Seo, W. S.; Lee, J. H.; Sun, X.; Suzuki, Y.; Mann, D.; Liu, Z.; Terashima, M.; Yang, P. C.; McConnell, M. V.; Nishimura, D. G.; Dai, H. *Nature Mat.* **2006**, *5*, 971–976.
- (5) Hayashi, Y.; Tokunaga, T.; Kaneko, K.; S. J. Henley, V. S.; Carey, J. D.; Silva, S. R. P. *IEEE Trans. on Nanotechnology* **2006**, *6*, 485–490.
- (6) Elías, A. L.; Rodríguez-Manzo, J. A.; McCartney, M. R.; Golberg, D.; Zamudio, A.; Baltazar, S. E.; López-Urías, F.; Muñoz-Sandoval, E.; Gu, L.; Tang, C. C.; Smith, D. J.; Bando, Y.; Terrones, H.; Terrones, M. *Nano Lett.* **2005**, *5*, 467–472.
- (7) Leonhardt, A.; Ritschel, M.; Kozhuharova, R.; Graffa, A.; Mühl, T.; Huhle, R.; Mönch, I.; Elefant, D.; Schneider, C. M. *Diamond Relat. Mater.* **2003**, *12*, 790–793.
- (8) Choi, W. Y.; Kang, J. W.; Hwang, H. J. *Phys. Rev. B* **2003**, *68*, 193405.
- (9) Bao, J.; Tie, C.; Xu, Z.; Suo, Z.; Zhou, Q.; Hong, J. *Adv. Mater.* **2002**, *14*, 1483–1486.
- (10) Bao, J.; Zhou, Q.; Hong, J.; Xu, Z. *Appl. Phys. Lett.* **2002**, *81*, 4592–4594.
- (11) Scott, J. H. J.; Majetich, S. A. *Phys. Rev. B* **1995**, *52*, 12564–12571.
- (12) Ruoff, R. S.; Lorents, D. C.; Chan, B.; Malhotra, R.; Subramoney, S. *Science* **1993**, *259*, 346–348.

- (13) Lokteva, E.; Kachevskii, S. A.; Turakulova, A. O.; Golubina, E. V.; Lunin, V. V.; Ermakov, A. E.; Uimin, M. A.; Mysik, A. A. *Russian J. Phys. Chem. A* **2009**, *83*, 1300–1306.
- (14) Ermakov, A. E.; Uimin, M. A.; Lokteva, E. S.; Mysik, A. A.; Kachevskii, S. A.; Turakulova, A. O.; Gaviko, V. S.; Lunin, V. V. *Russian J. Phys. Chem. A* **2009**, *83*, 1187–1193.
- (15) Huang, Y.; Xu, Z.; Yang, Y.; Tang, T.; Huang, R.; ; Shen, J. *J. Phys. Chem. C* **2009**, *113*, 6533–6538.
- (16) Galakhov, V. R.; Shkvarin, A. S.; Semenova, A. S.; Uimin, M. A.; Mysik, A. A.; Shchegoleva, N. N.; Yermakov, A. Y.; Kurmaev, E. Z. *J. Phys. Chem. C* **2010**, *114*, 22413–22416.
- (17) Artacho, E.; Gale, J. D.; García, A.; Junquera, J.; Martín, R. M.; Ordejón, P.; Sánchez-Portal, D.; Soler, J. M. *SIESTA, Version 1.3*; 2004.
- (18) Soler, J. M.; Artacho, E.; Gale, J. D.; García, A.; Junquera, J.; Ordejón, P.; Sánchez-Portal, D. *J. Phys.: Condens. Matter* **2002**, *14*, 2475.
- (19) Perdew, J. P.; Zunger, A. *Phys. Rev. B* **1981**, *77*, 5048–5079.
- (20) Yeh, J. J.; Lindau, I. *At. Data Nucl. Data Tables* **1985**, *32*, 1–155.
- (21) Cho, S.-J.; Kauzlarich, S. M.; Olamit, J.; Liu, K.; Grandjean, F.; Rebbouh, L.; Long, G. J. *J. Appl. Phys.* **2004**, *95*, 6804–6805.
- (22) Entani, S.; Ikeda, S.; Kiguchi, M.; Saiki, K. *Appl. Phys. Lett.* **2006**, *88*, 153126.
- (23) Pacilé, D.; Papagno, M.; Rodríguez, A. F.; Grioni, M.; Papagno, L.; Girit, Ç. Ö.; Meyer, J. C.; Begtrup, G. E.; Zettl, A. *Phys. Rev. Lett.* **2008**, *101*, 066806.
- (24) Coleman, V. A.; Knut, R.; Karis, O.; Grennberg, H.; Jansson, U.; Quinlan, R.; Holloway, B. C.; Sanyal, B.; Eriksson, O. *J. Phys. D: Appl. Phys.* **2008**, *41*, 062001.
- (25) Dedkov, Y. S.; Sicot, M.; Fonin, M. *J. Appl. Phys.* **2010**, *107*, 09E121.

- (26) Hua, W.; Gao, B.; Li, S.; Ågren, H.; Luo, Y. *Phys. Rev. B* **2010**, *82*, 155433.
- (27) Tang, Y. H.; Sham, T. K.; Hu, Y. F.; Lee, C. S.; Lee, S. T. *Chem. Phys. Lett.* **2002**, *366*, 636–641.
- (28) Jeong, H.-K.; Noh, H.-J.; Kim, J.-Y.; Glans, P.-A.; Jin, M. H.; Smith, K. E.; Lee, Y. H. *Phys. Rev. Lett.* **2009**, *102*, 099701.
- (29) Chastain, J. *Handbook of X-ray Photoelectron Spectroscopy*; Eden Prairie: Perkin Elmer Corporation, 1992.
- (30) Zajíčková, L.; Kučerová, Z.; Buršíková, V.; Eliáš, M.; Houdková, J.; Synek, P.; Maršíková, H.; Jašek, O. *Plasma Process. Polymers* **2009**, *6*, S864–S869.
- (31) Haiber, S.; Ai, X.; Bubert, H.; Heintze, M.; Brüser, V.; Brandl, W.; Marginean, G. *Anal. Bioanal. Chem.* **2003**, *130*, 875–883.
- (32) Jeong, H.-K.; Lee, Y. P.; Lahaye, R. J. W. E.; Park, M.-H.; An, K. H.; Kim, I. J.; Yang, C.-W.; Park, C. Y.; Ruoff, R. S.; Lee, Y. H. *J. Am. Chem. Soc.* **2008**, *130*, 1362–1366.
- (33) Jeong, H.-K.; Colakerol, L.; Jin, M. H.; Glans, P.-A.; Smith, K. E.; Lee, Y. H. *Chem. Phys. Lett.* **2008**, *460*, 499–502.
- (34) Jeong, H.-K.; Noh, H.-J.; Kim, J.-Y.; Jin, M. H.; Park, C. Y.; Lee, Y. H. *Europhys. Lett.* **2008**, *82*, 67004.
- (35) Giovannetti, G.; Khomyakov, P. A.; Brocks, G.; Karpan, V. M.; van den Brinkand, J.; Kelly, P. J. *Phys. Rev. Lett.* **2008**, *101*, 026803.
- (36) Stone, A. J.; Wales, D. J. *Chem. Phys. Lett.* **1986**, *128*, 501–503.
- (37) Skytt, P.; Glans, P.; Mancini, D. C.; Guo, J.-H.; Wassdahl, N.; Nordgren, J.; Ma, Y. *Phys. Rev. B* **1994**, *50*, 10457–10461.

- (38) Muramatsu, Y.; Hirono, S.; Umemura, S.; Ueno, Y.; Hayashi, T.; Grush, M. M.; Gullikson, E. M.; Perera, R. C. C. *Carbon* **2001**, *39*, 1403–1407.
- (39) Boukhvalov, D. W.; Karimov, P. F.; Kurmaev, E. Z.; Hamilton, T.; Moewes, A.; Finkelstein, L. D.; Katsnelson, M. I.; Davydov, V. A.; Rakhmanina, A. V.; Makarova, T. L.; Kopelevich, Y.; Chiuzbaian, S.; Neumann, M. *Phys. Rev. B* **2004**, *69*, 115425.
- (40) Ramm, M.; Ata, M.; Gross, T.; Unger, W. *Appl. Phys. A* **2000**, *70*, 387–390.
- (41) Boukhvalov, D. W.; Katsnelson, M. I. *Nano Lett.* **2008**, *8*, 4373–4379.
- (42) Lemme, M. C.; Bell, D. C.; Williams, J. R.; Stern, L. A.; Baugher, B. W. H.; Jarillo-Herrero, P.; Marcus, C. M. *ACS Nano* **2009**, *3*, 2674–2676.
- (43) Campos, L. C.; Manfrinato, V. R.; Sanchez-Yamagishi, J. D.; Kong, J.; Jarillo-Herrero, P. *Nano Lett.* **2009**, *9*, 2600–2604.
- (44) Boukhvalov, D. W.; Katsnelson, M. I. *Appl. Phys. Lett.* **2009**, *95*, 023109.